

Jaime G. Mancilla and Paul B. Manis

J Neurophysiol 102:1287-1295, 2009. First published May 27, 2009; doi:10.1152/jn.91272.2008

You might find this additional information useful...

This article cites 57 articles, 20 of which you can access free at:

<http://jn.physiology.org/cgi/content/full/102/2/1287#BIBL>

Updated information and services including high-resolution figures, can be found at:

<http://jn.physiology.org/cgi/content/full/102/2/1287>

Additional material and information about *Journal of Neurophysiology* can be found at:

<http://www.the-aps.org/publications/jn>

This information is current as of August 13, 2009 .

Two Distinct Types of Inhibition Mediated by Cartwheel Cells in the Dorsal Cochlear Nucleus

Jaime G. Mancilla and Paul B. Manis

Department of Otolaryngology/Head and Neck Surgery, University of North Carolina, Chapel Hill, North Carolina

Submitted 28 November 2008; accepted in final form 19 May 2009

Mancilla JG, Manis PB. Two distinct types of inhibition mediated by cartwheel cells in the dorsal cochlear nucleus. *J Neurophysiol* 102: 1287–1295, 2009. First published May 27, 2009; doi:10.1152/jn.91272.2008. Individual neurons have been shown to exhibit target cell-specific synaptic function in several brain areas. The time course of the postsynaptic conductances (PSCs) strongly influences the dynamics of local neural networks. Cartwheel cells (CWCs) are the most numerous inhibitory interneurons in the dorsal cochlear nucleus (DCN). They are excited by parallel fiber synapses, which carry polysensory information, and in turn inhibit other CWCs and the main projection neurons of the DCN, pyramidal cells (PCs). CWCs have been implicated in “context-dependent” inhibition, producing either depolarizing (other CWCs) or hyperpolarizing (PCs) post synaptic potentials. In the present study, we used paired whole cell recordings to examine target-dependent inhibition from CWCs in neonatal rat DCN slices. We found that CWC inhibitory postsynaptic potentials (IPSPs) onto PCs are large (1.3 mV) and brief (half-width = 11.8 ms), whereas CWC IPSPs onto other CWCs are small (0.2 mV) and slow (half-width = 36.8 ms). Evoked IPSPs between CWCs exhibit paired-pulse facilitation, while CWC IPSPs onto PCs exhibit paired-pulse depression. Perforated-patch recordings showed that spontaneous IPSPs in CWCs are hyperpolarizing at rest with a mean estimated reversal potential of -67 mV. Spontaneous IPSCs were smaller and lasted longer in CWCs than in PCs, suggesting that the kinetics of the receptors are different in the two cell types. These results reveal that CWCs play a dual role in the DCN. The CWC-CWC network interactions are slow and sensitive to the average rate of CWC firing, whereas the CWC-PC network is fast and sensitive to transient changes in CWC firing.

INTRODUCTION

The dorsal cochlear nucleus (DCN) is thought to play a role in determining the elevation of a sound source based on spectral cues (Oertel and Young 2004) and in the genesis of tinnitus (Kaltenbach 2006). Both roles depend on a cerebellar-like circuit in the molecular layer of the DCN, where nonauditory inputs converge with auditory inputs. Cells in the dorsal cochlear nucleus receive excitatory inputs from two main afferent systems. Auditory nerve afferents synapse on PCs and inhibitory interneurons in the deep layer of the DCN (Brown and Ledwith 1990; Kane 1974; Manis and Brownell 1983; Ryugo and May 1993). Afferents carrying information from somatosensory nuclei (Davis and Young 1997; Kanold and Young 2001; Shore 2005; Shore and Zhou 2006; Weinberg and Rustioni 1987; Zhou and Shore 2004), pontine nuclei (Ohlrogge et al. 2001), raphe nucleus (Thompson and Thompson 2001), type II spiral ganglion cells (Brown et al. 1988), auditory midbrain nuclei (Shore and Moore 1998), and audi-

tory cortex (Weedman and Ryugo 1996) synapse on granule cells. The granule cells in turn form the parallel fiber system that synapses on PCs and inhibitory interneurons in the superficial layer of the DCN.

The excitatory inputs, however, only account for about one-third of the synapses in the DCN. Two-thirds of the synaptic contacts in the DCN are inhibitory (Rubio and Juiz 2004), suggesting that inhibitory interneurons play a prominent role in the circuitry of the DCN. Cartwheel cells (CWCs) are the most numerous inhibitory interneuron class in the DCN and are likely responsible for a major portion of the inhibition onto PCs. However, the functional organization and synaptic dynamics of their inhibition is not clear. CWC axons remain within the DCN, synapsing with PCs and other cartwheel cells (Berrebi and Mugnaini 1991; Manis et al. 1994). CWCs are similar to cerebellar Purkinje cells in that they fire complex spike bursts as well as simple spikes (Kim and Trussell 2007; Manis et al. 1994; Zhang and Oertel 1993). Physiological studies suggest that CWCs use glycine as their principal transmitter (Golding and Oertel 1997; Zhang and Oertel 1993), although many CWCs also stain for GABA and the precursor for GABA, glutamic acid decarboxylase (GAD) (Altschuler et al. 1986; Campos et al. 2001; Juiz et al. 1989; Kolston et al. 1992; Rubio and Juiz 2004; Wenthold et al. 1986). The role that GABA plays in the synaptic transmission of CWCs is unknown; however, in the medial nucleus of the trapezoid body, it serves to speed up glycinergic transmission (Lu et al. 2008). In mice, CWC-mediated IPSPs in PCs have been shown to be hyperpolarizing in an age range of P18–26, whereas those in CWCs have been shown to be depolarizing in the same age range (Golding and Oertel 1996, 1997). However, in guinea pigs, likely CWC inhibitory postsynaptic potentials (IPSPs) in other CWCs were reported to be hyperpolarizing (Manis et al. 1994).

We examined CWC-mediated inhibition in the DCN, using paired whole cell recordings and perforated-patch recordings, in a rat cochlear nucleus brain slice preparation. We provide direct evidence of CWC-mediated IPSPs onto PCs and CWCs. We found that CWC IPSPs onto other CWCs are weak and facilitating, whereas those onto PCs are strong and depressing. In addition, CWC evoked IPSPs in PCs are significantly briefer than those in CWCs. Perforated-patch recordings showed that CWCs received hyperpolarizing spontaneous IPSPs at rest, which reversed near -67 mV. Spontaneous IPSCs were smaller and lasted longer in CWCs than in PCs, suggesting that the kinetics of the receptors are different in the two cell types.

Address for reprint requests and other correspondence: P. B. Manis: Dept. of Otolaryngology/HNS, Physician Office Building, 170 Manning Dr., C.B. 7070, University of North Carolina, Chapel Hill, NC 27599-7070 (E-mail: pmanis@med.unc.edu).

METHODS

Sprague-Dawley rat pups, 9–18 days old, were used in the present experiments. All experimental protocols were approved by the University of North Carolina at Chapel Hill Internal Animal Care and Use Committee. Rats were anesthetized with 100 mg/kg ketamine and 10 mg/kg xylazine until areflexic. The brain was then harvested in 34°C, low calcium-high magnesium, artificial cerebrospinal fluid (ACSF) composed of (in mM): 122 NaCl, 3 KCl, 1.25 KH₂PO₄, 25 NaHCO₃, 10 glucose, 3 myo-inositol, 2 Na-pyruvate, 0.4 ascorbic acid, 3.7 MgSO₄, and 0.1 CaCl₂ and saturated with 95% O₂-5% CO₂. The cochlear nucleus was isolated, and slices 250 μm thick were prepared on a Leica VT1000 slicer, in the transstrial plane (Blackstad et al. 1984). Slices were placed in an incubation chamber at 34°C containing the standard ACSF (same as dissection except 1.5 mM MgSO₄ and 2.5 mM CaCl₂ were used), the slice chamber was then transferred to room temperature and kept at that temperature. Recordings were done at 34°C in the standard ACSF.

Patch pipettes were made from 1.5 mm KG-33 glass (Garner, Claremont, CA) and filled with (in mM) 126 K-gluconate, 6 KCl, 2 NaCl, 10 HEPES, 0.2 EGTA, 4 ATP-Mg, 0.3 GTP-Tris, and 10 phosphocreatine-Tris. The pH was adjusted to 7.25 with KOH, and the osmolarity was set to 295 mOsm. For perforated-patch experiments, the electrode solution consisted of (in mM) 140 KCl, 10 NaCl, 10 HEPES, and 10 mM sucrose. The tips of the pipettes were filled with this internal and backfilled with the same solution containing 5 μg/ml of gramicidin (Sigma-Aldrich) in DMSO (Kim and Trussell 2007; Lohrke et al. 2005). In some experiments, fast glutamatergic transmission was blocked with 5 μM CNQX and 50 μM D-2-amino-5-phosphonovaleric acid (D-APV) or 2.0 mM kynurenic acid (Tocris). Glycinergic IPSCs were blocked with strychnine (2 μM; Sigma-Aldrich). Sodium-dependent action potentials were blocked with 0.5 μM TTX.

Whole cell recordings and cell-attached recordings were obtained under IR-DIC using a Zeiss FS-2 microscope, and a Multiclamp 700A amplifier (MDS Analytical Technologies, Toronto, Ontario, Canada). Data were collected using a program written in MATLAB (The Mathworks, Natick, MA).

Data analysis

Data were analyzed using programs written in MATLAB and Labview (National Instruments, Austin, TX). Spontaneous IPSPs and IPSCs were selected using a template matching algorithm (Clements and Bekkers 1997). The resting membrane potential (RMP) of pyramidal cells was measured with 0-pA holding current. Cartwheel cells were spontaneously active and thus did not have a true RMP. For these cells, we determined the minimum holding current needed to suppress firing and then measured the membrane potential at this holding current. The input resistance (R_{in}) was measured from the slope of the linear portion of the subthreshold current-voltage (I - V) plot. The peak of the second derivative of the voltage was used to identify the action potential threshold. Additional measurements were made of the action potential amplitude, time to peak, afterhyperpolarization depth, and width at half height. All voltages reported were adjusted for a junction potential of -12 mV, except for perforated-patch experiments, where no correction was made. Data are reported as means ± SD. All comparisons were made using a two-tailed unpaired t -test.

The membrane potential of simultaneously recorded cells was cross-correlated to identify common fluctuations. The voltage was sampled at 10 kHz and normalized by the SD (Beierlein et al. 2000)

$$\frac{\sum V_1(t) \cdot V_2(t)}{(s.d.V_1(t)) \cdot (s.d.V_2(t))}$$

RESULTS

Properties of pyramidal cells and CWCs

Pyramidal cells (PCs) in the DCN were distinguished from CWCs by soma shape and by their responses to depolarizing current pulses (Fig. 1). PCs had large, often fusiform-shaped, cell bodies and fired simple action potentials in response to depolarizing current pulses (Manis 1990; Zhang and Oertel 1994), whereas CWCs had small cell bodies and fired complex action potentials (Golding and Oertel 1997; Kim and Trussell 2007; Manis et al. 1994; Molitor and Manis 2003; Zhang and Oertel 1993). PCs had a mean resting membrane potential of -63 ± 8 mV ($n = 38$). The membrane potential of CWCs oscillates, and action potentials arise from the peak of the oscillations making it difficult to determine a true RMP. When a small holding current (-45 ± 53 pA) was injected, oscillations ceased and a quiescent membrane potential of -62 ± 8 mV ($n = 58$) could be measured. Action potential half-width ($P = 1.9 \times 10^{-6}$), amplitude ($P = 6.5 \times 10^{-15}$), and afterhyperpolarization ($P = 6.9 \times 10^{-5}$), as well as the input resistance (R_{in} ; $P = 1.0 \times 10^{-15}$) and membrane time constant (τ_m ; $P = 0.01$) of PCs, were all significantly different from those of CWCs (see Table 1), as previously reported for guinea pig cells (Manis et al. 1994).

Dual recordings

EVOKED IPSPs. To study synaptic interactions between defined sets of cells in the DCN, dual whole cell recordings were made from PC and CWC pairs ($n = 17$), CWC pairs ($n = 11$), or PC pairs ($n = 2$). Action potentials in CWCs produced IPSPs in nearby PCs (11/17 pairs) and in nearby CWCs (6/11 pairs). Three of the connected CWC-CWC pairs had bidirectional connections. We measured the distance between the centers of the cell bodies of cells in a pair using an image obtained with the $\times 40$ objective under IR-DIC (see Fig. 1). For pairs that were too far apart to measure with the $\times 40$ objective, or that did not have an image captured at high magnification, distances were estimated from images taken at a lower magnification. The probability of connection for CWC-PC pairs was higher when cells were within 50 μm of each other (73%; $n = 11$) than when the distance between cells was >50 μm (40%; $n = 5$). The largest distance we observed for a connected pair was 150 μm. For CWC-CWC pairs that were within 50 μm, the

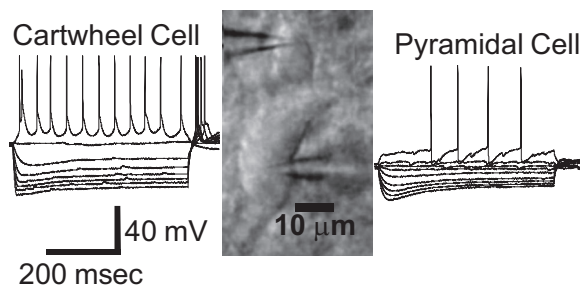


FIG. 1. Whole cell current-clamp recordings of a cartwheel cell (CWC, left) and a pyramidal cell (PC, right), in the dorsal cochlear nucleus, showing their typical membrane voltage responses to current steps. The CWC from which the traces were obtained is the small cell at the top of the IR-DIC image shown in the center. The PC is the larger cell in the bottom with the pipette coming from the right. The resting membrane potential for the CWC was -68 mV, whereas that for the PC was -69 mV.

TABLE 1. *Intrinsic electrophysiological properties of PCs and CWCs*

	PC	<i>n</i>	CWC	<i>n</i>
R_{in} , M Ω	64 \pm 21*	38	187 \pm 78	64
τ_m	21 \pm 8*	38	17 \pm 7	64
AP Threshold, mV	-50 \pm 9	38	-50 \pm 9	64
AP Amplitude, mV	76 \pm 9*	38	55 \pm 12	64
AP HW, ms	0.7 \pm 0.1*	38	1.1 \pm 0.4	64
AP TTP, ms	0.7 \pm 0.4	38	0.8 \pm 0.4	64
AHP Depth, mV	13 \pm 2*	38	8 \pm 7	64

Intrinsic electrophysiological properties of PCs and CWCs reported as means \pm SD. Input resistance (R_{in}), membrane time constant (τ_m), action potential threshold, action potential amplitude, action potential half-width (AP HW), action potential time to peak (AP TTP) and action potential afterhyperpolarization depth (AHP Depth). The AP threshold and time to peak of pyramidal cells (PCs) were not significantly different from those of cartwheel cells (CWCs) ($P > 0.01$). Significantly different parameters are marked with an asterisk.

probability of at least a unidirectional connection was 75% (6/8). On the other hand, even with trains of action potentials, PCs never produced PSPs in nearby PCs (0/2 pairs) or CWCs (0/17 pairs). This is consistent with the anatomical observations that PCs in rodents do not have axon collaterals within the DCN itself (Manis 1990; Zhang and Oertel 1993). These data suggest that only cells closer together than $\sim 100 \mu\text{m}$ are likely to be connected, consistent with the limited spatial domains of individual CWC axons (Manis et al. 1994), and that CWCs are just as likely to be connected to nearby PCs as they are to other CWCs.

Inhibitory interneurons in cortex (Reyes et al. 1998) and cerebellum (Dugue et al. 2005) have been shown to exhibit target-cell-dependent synaptic inhibition. To determine whether this is the case in the DCN, we compared IPSPs produced by CWCs in other CWCs and in PCs. Action potentials in CWCs produced IPSPs in nearby CWCs with mean amplitudes of 0.2 ± 0.2 mV ($n = 9$). IPSPs were slow, with a mean time to peak of 12.0 ± 6.7 ms, a mean time constant for the rising phase (τ_r) of 8.8 ± 4.8 , and a mean width at half height (half-width) of 36.8 ± 18.1 ms ($n = 9$). In contrast, IPSPs in nearby PCs were larger and faster than those in CWCs with a mean amplitude of 1.3 ± 0.9 mV, mean time to peak of 3.3 ± 1.1 ms, mean τ_r of 1.0 ± 0.6 , and a mean half-width of 11.8 ± 8.6 ms (all $n = 11$ except for half-width $n = 10$). The amplitudes ($P = 0.003$), time to peak ($P = 1.0 \times 10^{-4}$), τ_r ($P = 4.2 \times 10^{-5}$) and half-width ($P = 0.001$) of evoked IPSPs in PCs were significantly different than those in CWCs. Figure 2 shows mean IPSPs for a CWC-CWC (A) and a CWC-PC (B) pair and the corresponding presynaptic action potentials. The membrane potential at which the IPSPs were collected had a small effect on the amplitude of IPSPs but did not account for the difference in amplitude between CWCs and PCs (Fig. 2C).

The different amplitudes of IPSPs in CWC and PCs suggested that release probability might differ at the two sets of target synapses. To further investigate this idea, we examined the dynamics of synaptic transmission in response to trains of action potentials. CWC-CWC synapses exhibited modest paired-pulse facilitation (P2/P1: 1.8 ± 1.5 ; $n = 6$), whereas CWC-PC synapses exhibited strong paired-pulse depression (P2/P1: 0.7 ± 0.2 ; $n = 10$). With repeated stimulation at 10 Hz, the majority of the depression of IPSPs in the CWC-PC pairs

occurred by the third action potential in the train with little depression thereafter (Fig. 2D). The mean coefficient of variation (CV) for the amplitude of single IPSPs in CWC-PC pairs was 0.71 ± 0.06 . In the CWC-CWC pairs, facilitation was maximal by the second presynaptic action potential, and the IPSP amplitude thereafter was either constant or slightly decreased (Fig. 2D). The mean CV for the amplitude of IPSPs in CWC-CWC pairs was 0.75 ± 0.23 . While the variance of the amplitude of IPSPs in CWC-PC and CWC-CWC pairs was significantly different for the first pulse ($P = 1.5 \times 10^{-4}$), it was not significantly different for all the pulses after the first pulse ($P > 0.01$; 2-tailed *F*-test). For the CWC-PC pairs, IPSPs had consistent time to peak with small variability throughout the 10 Hz train. The mean CV for the time to peak of IPSPs in CWC-PC pairs was 0.3 ± 0.06 . The time to peak of CWC-CWC pairs were more variable than those of CWC-PC pairs and showed a slight decrease throughout the 10-Hz train (Fig. 2E). The mean CV for the time to peak of IPSPs in CWC-CWC pairs was 0.5 ± 0.06 . The variance of the time to peak of IPSPs was significantly different for CWC-PC and CWC-CWC pairs ($P < 0.01$; 2-tailed *F*-test). As can be seen from Fig. 3,

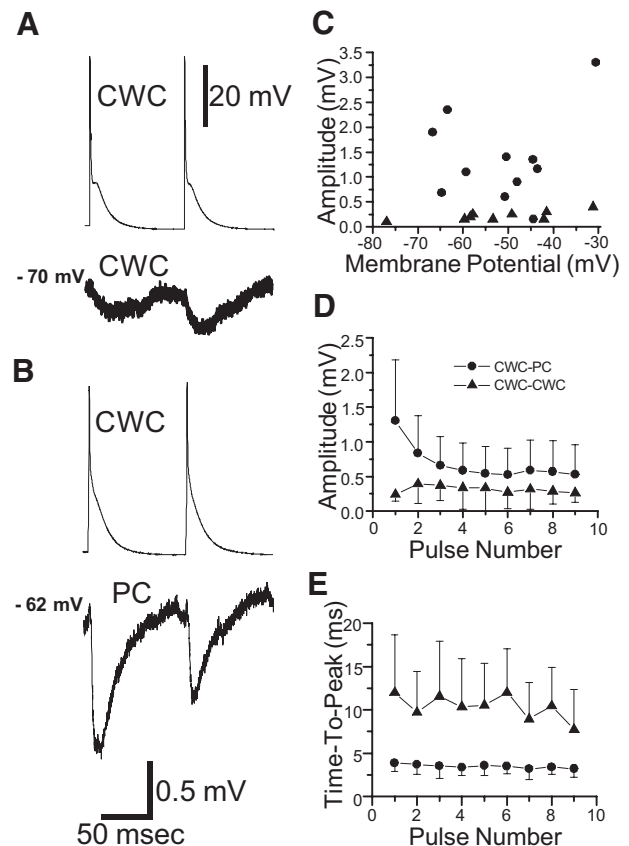


FIG. 2. Trains of action potentials in CWCs produced inhibitory postsynaptic potentials (IPSPs) in nearby CWCs and PCs. *A*: mean IPSPs and the corresponding presynaptic action potentials for a CWC-CWC pair. The membrane potential at which the IPSPs were collected is noted. *B*: mean IPSPs and the corresponding presynaptic action potentials for a CWC-PC pair. *C*: amplitude of IPSPs in CWC-PC (●) and CWC-CWC (▲) pairs as a function of the membrane potentials at which the IPSPs were collected. *D*: mean \pm SD amplitudes of IPSPs for 10 CWC-PC and 6 CWC-CWC pairs showing depression of IPSPs in the CWC-PC pairs and facilitation in the CWC-CWC pairs. *E*: mean time to peak \pm SD of IPSPs for 10 CWC-PC and 6 CWC-CWC pairs showing small variability in time to peak for CWC-PC pairs and large variability for CWC-CWC pairs.

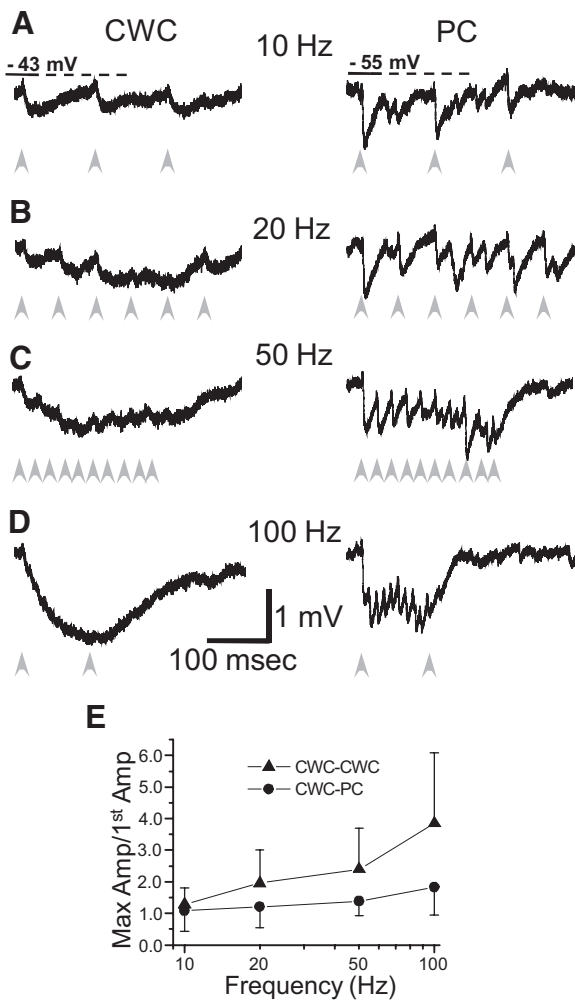


FIG. 3. Trains of IPSPs in CWCs and PCs evoked by action potentials in presynaptic CWCs. *A*: 10-Hz train of IPSPs in a CWC-CWC pair (left) and in a CWC-PC pair (right). *B*: 20-Hz trains of IPSPs. *C*: 50-Hz trains of IPSPs, showing a greater degree of summation in the CWC than in the PC. *D*: 100-Hz train of IPSPs, showing that individual IPSPs summate to produce a large hyperpolarization in the CWC and a smaller hyperpolarization in the PC. *E*: population means for CWC-PC (●) and CWC-CWC (▲) pairs showing a higher degree of summation in CWC-CWC pairs. The maximum summation during the trains divided by the amplitude of the 1st pulse is plotted as a function of frequency. ---, the membrane potential at which the IPSPs in *A–D* were collected. ↑, the timing of presynaptic action potentials. ↑ in *D* indicate the 1st and last presynaptic action potential.

low-frequency (10–20 Hz) trains produce little summation of IPSPs in CWC-CWC and CWC-PC pairs. However, at higher frequencies (50–100 Hz), IPSPs summate to produce a large hyperpolarization (Fig. 3, *C* and *D*). This summation was seen in all six of the connected CWC-CWC pairs tested. In CWC-PC pairs, summation varied but never reached the magnitude of summation in CWC-CWC pairs. This can be seen in the population average shown in Fig. 3*E*, which plots the maximum amplitude of the summation divided by the amplitude of the first pulse as a function of the frequency of stimulation. Paired-pulse depression of IPSPs in CWC-PC pairs, and IPSP summation in both CWC-PC and CWC-CWC pairs, was augmented by the burst firing of CWCs. Figure 4 shows the effect of burst firing in both CWC-PC and CWC-CWC pairs. The black traces are averages of trials in which the presynaptic CWC fired simple action potentials. The average

IPSP and action potential shown for the CWC-PC pair (Fig. 4*A*) is the first action potential in a 10-Hz train of action potentials. The average action potential shown for the CWC-CWC pair (Fig. 4*B*) was not obtained from a 10-Hz train, but instead, from 500-ms current injection pulses. The red traces are the average of trials in which the presynaptic CWC fired a burst of two or more action potentials. As can be seen, the burst firing enhanced the amplitude and duration of IPSPs in both PCs and CWCs. Because CWCs are more likely to produce a burst of action potentials at the start of an episode of spontaneous firing (Portfors and Roberts 2007), the paired pulse ratio for CWC-PC pairs during spontaneous firing will be higher than that seen with trains of action potentials. The burst firing will also tend to increase the summation of IPSPs because of an increased duration of the first IPSP. The dynamics of CWC inhibition appears to be complex and varies in accordance to the target cell and the mode of action potential firing in the presynaptic CWC.

SPONTANEOUS IPSPs. Close inspection of simultaneously recorded voltage traces of spontaneous activity indicated that individual IPSPs in one cell of a pair were likely to be correlated in time with IPSPs in the other cell (Fig. 5*A*). Because we did not block spontaneous spiking in the slice, the simultaneous IPSPs most likely arose from shared inputs from a third cell that was firing spontaneously. To more rigorously identify which cell pairs had shared input, we calculated the cross-correlation of simultaneously recorded membrane potentials from pairs of cells (see METHODS). Five of the seven CWC-PC pairs and one of the four CWC-CWC pairs had peaks in the correlogram near zero time, suggesting the presence of one or more shared inputs to the recorded cell pair. Figure 5*B* shows the mean correlogram of the membrane potential averaged from 16 5-s traces in one CWC-PC pair. The maximum correlation coefficient was 0.32 suggesting a strong correlation of the inputs to the two cells of the pair. The mean maximum correlation coefficient for the five CWC-PC pairs was $0.21 \pm$

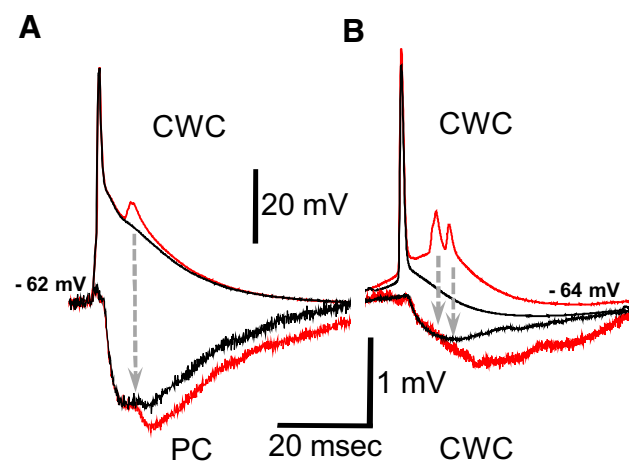


FIG. 4. Comparison of IPSPs produced by single action potentials (black traces) in CWCs with those produced by a burst of action potentials (red traces). Arrows indicate the timing of the action potentials in the burst. *A*: CWC-PC pair showing the mean of single action potentials and the mean IPSP from the single action potentials in black, whereas the mean burst and mean IPSP resulting from the burst are shown in red. *B*: CWC-CWC pair showing the mean single action potential and mean IPSP resulting from the action potential in black, whereas the mean burst and mean IPSP resulting from the burst are shown in red.

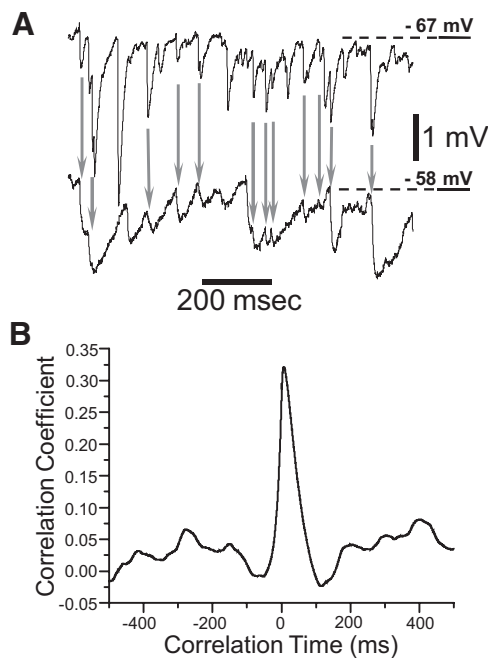


FIG. 5. Traces of ongoing activity were collected in a CWC-PC pair to perform a cross-correlation analysis on the membrane potentials. *A*: simultaneously recorded traces for each of the cells in the pair. \downarrow , the IPSPs that occurred within 1 ms of each other in the 2 cells. ---, the RMP of the cells. *B*: the mean correlogram of the membrane potential for 16 5-s traces in this pair had a maximum correlation coefficient of 0.32, which occurred with a delay of 7 ms.

0.08. The CWC-CWC pair had a maximum correlation coefficient of 0.12, indicating that the shared input to the pair did not contribute as much to the membrane potential as in the CWC-PC pairs.

Ongoing spontaneous synaptic events were further analyzed in the five CWC-PC pairs. Figure 5*A* shows simultaneously recorded traces for a PC (*top trace*) and a CWC (*bottom trace*) of one of the pairs; IPSPs that occurred within 1 ms are indicated (\downarrow). The amplitudes of simultaneously occurring IPSPs, which were selected as indicated in Fig. 5*A*, were not correlated between CWCs and PCs (Fig. 6*A*). Figure 6 shows the amplitude, time to peak, and half-widths for simultaneous IPSPs in the CWC-PC pairs that had peaks in the correlograms near 0 time (6.0 ± 2.5 ms). The mean amplitude for IPSPs in the CWCs was 1.1 ± 0.3 mV, whereas that for IPSPs in the PCs was 2.0 ± 0.4 mV. In addition, IPSPs in PCs were faster than those in CWCs (Fig. 6*B*). The times to peak of IPSPs in the CWCs (\circ) were longer than those in the PCs (\bullet) and were positively correlated with the amplitude of IPSPs. Time to peak of IPSPs in the PCs remained relatively constant regardless of the amplitude of the IPSPs. The mean time to peak of IPSPs in the CWCs was 12.3 ± 1.0 ms while that in the PCs was 3.9 ± 0.7 ms. Half-widths of IPSPs in the CWCs (\circ) showed a similar trend as the time to peak; they were longer than those of IPSPs in the PC (\bullet) and were positively correlated with the amplitude of IPSPs (Fig. 6*C*). Like the time to peak of IPSPs in the PCs, the half-widths of IPSPs in the PCs remained relatively constant regardless of the amplitude. The mean half-width of IPSPs in the CWCs was 36.5 ± 2.8 ms, whereas that in the PCs was 18.5 ± 5.0 ms. These measurements are

consistent with those obtained in CWCs and PCs with direct presynaptic stimulation of CWCs.

Reversal potential of CWC IPSPs

In the experiments described in the preceding text, the IPSP reversal potential was established by the internal Cl^- concentration of the recording pipette. However, it has been reported that CWCs may have high internal Cl^- until at least postnatal day 21 such that IPSPs are depolarizing. To determine whether the Cl^- reversal was more depolarized than the resting membrane potential of CWCs, we examined IPSPs in CWCs in which the internal Cl^- concentration was unperturbed using gramicidin-perforated-patch recordings ($n = 9$). The spontaneous IPSPs were always hyperpolarizing at the resting membrane potential (-52.6 ± 2.9 mV) with a mean amplitude of 1.9 ± 1.1 mV. The mean time to peak of IPSPs was 16.8 ± 4.1 ms, and the mean half-width was 32.9 ± 11.5 ms, similar to the results seen in whole cell recordings. The gray trace in Fig. 7*A* shows the hyperpolarizing IPSPs at the resting membrane potential (-48 mV) of one of the cells studied. This data were collected in rats ranging in age from P10 to P12 and suggests that inhibitory inputs to CWCs have already switched from depolarizing to hyperpolarizing at these ages.

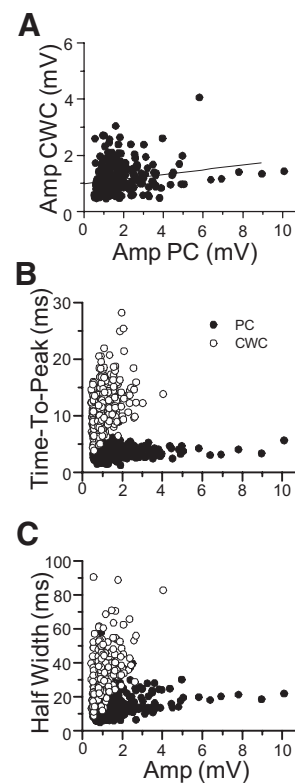


FIG. 6. Measurements of simultaneously occurring IPSPs for 5 CWC-PC pairs with peaks near 0 in the correlograms. *A*: amplitudes of simultaneously occurring IPSPs are uncorrelated. ---, the best fit to the data. *B*: times to peak of IPSPs in the CWCs (\circ) are longer than those in the PCs (\bullet) and increase with increases in the amplitude of IPSPs. Time to peak of IPSPs in the PCs remain relatively constant regardless of the amplitude of the IPSPs. *C*: half-widths of IPSPs in the CWCs (\circ) showed a similar trend as the time to peak; they were longer than those of IPSPs in the PCs (\bullet) and increased with increases in amplitude. Like the time to peak of IPSPs in the PCs, the half-widths of IPSPs in the PCs remained relatively constant regardless of the amplitude.

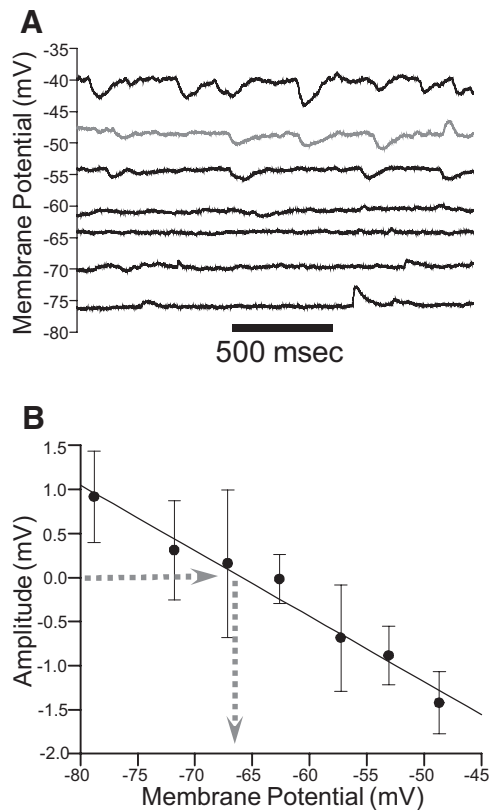


FIG. 7. Reversal potential analysis for IPSPs recorded with perforated-patch recordings. *A*: voltage traces obtained with current steps of different amplitudes. IPSPs are seen at the resting membrane potential (gray trace) and at more hyperpolarized and depolarized membrane potentials. *B*: mean amplitudes for IPSPs collected in 3 cells at several different membrane potentials. Dashed lines indicate the reversal potential of the IPSPs.

The time course of the spontaneous IPSPs, collected in pairs with correlated inputs and also in cells studied with the perforated-patch recordings, is similar to the time course of evoked IPSPs in CWC-PC and CWC-CWC pairs, suggesting that the shared input in the CWC-PC pairs comes from other spontaneously active CWCs.

Because the perforated-patch recordings showed that IPSPs in CWCs were hyperpolarizing at -53 mV, we measured the reversal potential of spontaneous IPSPs in three cells. To isolate the inhibitory inputs, we blocked fast glutamatergic transmission with 5 μ M CNQX and 50 μ M APV. Postsynaptic potentials were detected using a template-matching algorithm (Clements and Bekkers 1997) that was run once to detect hyperpolarizing events and a second time to detect depolarizing events. The mean estimated reversal potential from P10-11 rats was -66.7 ± 8.4 mV ($n = 3$). The mean amplitude of IPSPs at different membrane potentials is plotted in Fig. 7*B*. Using the amplitudes measured at the lowest and highest membrane potential only, which are well above the noise for the recordings, gives an estimated reversal potential of -67.7 ± 8.5 mV. These estimates of the reversal potential are negative to the resting membrane potential of CWC and suggest that inhibition is hyperpolarizing in CWCs at rest. Taken together, the data from paired recordings provides the first description of CWC evoked IPSPs onto PCs and other CWCs, suggests that IPSPs are faster in PCs than in CWCs, and that

already at P10 IPSPs are hyperpolarizing at resting membrane potentials in rat CWCs.

Spontaneous IPSCs

We consistently observed that IPSPs in CWCs and PCs had a different time course. This could occur if the underlying synaptic conductance had different kinetics or if the voltage changes driven by the synaptic conductance, with the same (or similar) kinetics, were being shaped by the postsynaptic cell. To discriminate between these possibilities, we measured the kinetics of spontaneous inhibitory postsynaptic currents (IPSCs) in PCs and CWCs under voltage clamp. Figure 8 shows the current trace for a PC (*A*) and a CWC (*B*) at a holding potential of -62 mV. The IPSCs that we measured were synaptically driven by the spontaneous activity of inhibitory interneurons in the slice. This was evident by the lack of IPSCs when we blocked glutamatergic receptors and action potentials with 2.0 mM kynurenic acid and 0.5 μ M TTX, respectively ($n = 5$). We measured the amplitude ($P = 2.8 \times 10^{-4}$), time to peak ($P = 0.02$), half-width ($P = 0.002$), τ_r ($P = 0.09$), and τ_f ($P = 0.005$) of IPSCs in PCs ($n = 17$) and CWCs ($n = 15$) and found that the amplitude and time course of IPSCs in PCs were significantly larger and shorter, respectively, than those of IPSCs in CWCs (Table 2). The mean IPSC for a PC (red trace) and a CWC (black trace) are overlaid in Fig. 8*C* to illustrate the difference in time course. The rising phase of IPSCs in the two cell types was not significantly different, but the decay phase of IPSCs was slower in CWCs. The wider half-width and slower τ_f of IPSCs in CWCs were not correlated with the amplitude of

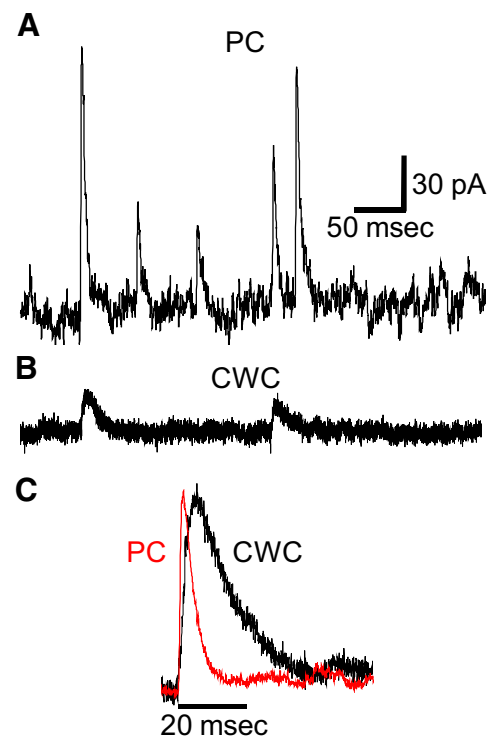


FIG. 8. Current traces showing IPSCs obtained at a holding potential of -62 mV. *A*: IPSCs obtained from a PC are large and fast. *B*: IPSCs obtained from a CWC are smaller and slower than those in the PC. *C*: normalized mean IPSC for the same PC (red trace) shown in *A* and for the same CWC (black trace) shown in *B*.

TABLE 2. Mean IPSC parameters for CWCs and PCs

	PC (<i>n</i> = 17)	CWC (<i>n</i> = 15)
Amplitude, pA	66 ± 24*	36.3 ± 16.4
HW, ms	5.0 ± 2*	8.1 ± 3.0
TTP, ms	1.5 ± 0.5	2.1 ± 1.0
τ_r	0.9 ± 0.7	1.4 ± 0.9
τ_f	5.6 ± 3.3*	10.0 ± 4.8

Amplitude, width at half height (HW), time to peak (TTP), rising time constant (τ_r), and falling time constant (τ_f) are given as means ± SD. Significantly different parameters are marked with an asterisk ($P < 0.01$). Number of cells is in parentheses. IPSC, inhibitory postsynaptic current.

IPSCs because the difference between PCs and CWCs remained when only IPSCs with matching amplitudes of 50–60 pA were compared.

To determine if there was an age-related change in the glycinergic receptors, we compared IPSCs from P12 to P14 animals against those from P16 to P18 animals in PCs and CWCs. We found no significant difference ($P > 0.05$) in any of the measures between the IPSC shape of PCs and CWCs in these two age ranges.

While CWCs use glycine as their principal transmitter, they may also release GABA (Altschuler et al. 1986; Campos et al. 2001; Juiz et al. 1989; Kolston et al. 1992; Rubio and Juiz 2004; Wenthold et al. 1986). To test the contribution of GABA receptors to the CWC-mediated IPSCs, we recorded spontaneous IPSCs in the presence of the glycinergic antagonist strychnine. The frequency of spontaneous IPSCs decreased from 5.6 Hz in a PC under control conditions to 0.1 Hz after the bath application of 2 μ M strychnine. Similarly in CWCs, the event frequency fell from 1.8 Hz under control conditions to 0.3 Hz after the bath application of strychnine ($n = 13$). These results suggest that the GABAergic contribution to the spontaneous events recorded is small, and is consistent with previous reports of spontaneous synaptic activity in CWCs and PCs (Golding and Oertel 1997) and evoked IPSPs in CWCs (Roberts et al. 2008).

DISCUSSION

Electrical parameters of PCs and CWCs

In this study, we differentiated CWCs from PCs by their firing pattern and the size and shape of their cell bodies. This was possible because in the DCN only CWCs fire bursts of action potentials (Golding and Oertel 1997; Kim and Trussell 2007; Manis et al. 1994; Molitor and Manis 2003; Zhang and Oertel 1993), whereas PCs fire only simple action potentials (Manis 1990; Zhang and Oertel 1994). In addition, CWC action potentials have longer falling phases and wider half-widths than those in PCs (Manis 1990; Manis et al. 1994). CWCs and PCs also cluster into different groups when separated by the size of their cell bodies (Manis et al. 1994). CWCs have small round or ovoid cell bodies (Berrebi and Mugnaini 1991; Brawer et al. 1974; Manis et al. 1994; Wouterlood and Mugnaini 1984; Zhang and Oertel 1993), whereas PCs have large fusiform cells bodies (Berrebi and Mugnaini 1991; Brawer et al. 1974; Manis 1990; Manis et al. 1994; Osen 1969; Zhang and Oertel 1994). We found, that in addition to the physiological differences stated in the preceding text, the action potential amplitude, the depth of the action potential afterhyperpolarization, the membrane time constant, and the

input resistance of CWCs were all significantly different from those of PCs in rats, consistent with previous observations in guinea pig (Manis et al. 1994) and mouse (Kim and Trussell 2007; Zhang and Oertel 1993).

IPSP shape

We provide the first direct evidence of CWC-mediated IPSPs onto PCs and quantify CWCs IPSPs onto other CWCs. We showed that the amplitude, time to peak, τ_r , and half-width of evoked IPSPs in PCs were significantly different from those in CWCs ($P < 0.01$). Previously, the source of IPSPs in CWCs and PCs was assumed to be other CWCs. This assumption was based on evidence from putative synaptic contacts at the light microscopic level (Manis et al. 1994), synaptic contacts at the electron microscopic level (Berrebi and Mugnaini 1991; Wouterlood and Mugnaini 1984), and indirect physiological evidence (Golding and Oertel 1996, 1997). Our data suggest that a majority of IPSPs seen in both CWCs and PCs, in the slice, arise from spontaneous firing of CWCs. We also found that action potentials in PCs did not produce postsynaptic responses in either CWCs or other PCs. This is consistent with anatomical evidence that suggests that PCs are projection neurons and do not have axon collaterals within the DCN (Manis 1990; Oertel and Wu 1989).

Correlated spontaneous IPSPs in simultaneously recorded CWC-PC pairs indicate that a single CWC produces IPSPs with different time courses depending on the target cell. That the presynaptic cell producing the correlated IPSPs is a CWC is supported by the similarity in shape parameters of the correlated IPSPs and those of CWC-evoked IPSPs. This is further reinforced by anatomical evidence that suggests that single CWCs could inhibit both PCs and other CWCs (Manis et al. 1994; Wouterlood and Mugnaini 1984).

To determine whether the difference in IPSP shapes between CWCs and PCs was due to differences in the underlying synaptic currents, we studied ongoing IPSCs in voltage-clamp experiments. We found that IPSCs in CWCs were significantly smaller and lasted longer than those in PCs. We also found that the majority of IPSCs in PCs were produced by action potential-mediated release from spontaneously active inhibitory interneurons in the slice rather than from spontaneous quantal release. In addition, PCs had a higher frequency of IPSCs than CWCs. This suggests that PCs receive connections from more CWCs than CWCs. The difference in IPSP shape between PCs and CWCs is not due to differences in the intrinsic membrane properties of PCs and CWCs. Two of the membrane properties we measured tend to oppose the difference in amplitude and time course that we observed in the two cell types. The CWCs we recorded from were smaller than the PCs and had larger R_{in} . For the same synaptic conductance change and synapse location, this difference in R_{in} would tend to produce larger IPSPs in CWCs. The assumption of a similar distribution of synaptic endings from CWCs on both CWCs and PCs is supported by anatomical studies that indicate that they both receive synaptic terminals from CWCs on their cell bodies and proximal dendrites (Berrebi and Mugnaini 1991; Manis et al. 1994; Rubio and Juiz 2004). In addition, the τ_m of CWCs was slightly but significantly shorter than that in PCs. This would tend to produce faster IPSPs in CWC.

The difference in time course of IPSPs is most likely the result of differences in the kinetics of the postsynaptic glycinergic receptors, as suggested by the difference in IPSC time course between the PCs and CWCs and the consistent block of spontaneous IPSCs by strychnine. The difference in IPSC kinetics is probably not a consequence of a developmental switch from $\alpha 2$ to $\alpha 1$ subunits in the glycine receptors of PCs and CWCs because the $\alpha 2$ subunit is expressed at very low levels in the cochlear nucleus, even at birth. Postnatal glycinergic receptors in the cochlear nucleus use predominantly the $\alpha 1$ subunit (Piechotta et al. 2001; Sato et al. 1995, 2000). The $\alpha 3$ subunit might be differentially distributed in the two cell types, but its expression has only been studied in PCs and not in CWCs (Piechotta et al. 2001). The $\alpha 3$ subunit has lower affinity for strychnine and is less sensitive to glycine than the $\alpha 1$ subunit, which would suggest that CWCs might have higher ratios of $\alpha 3/\alpha 1$ subunits than PCs. Most of the cells we recorded from came from animals that ranged in age from P12 to P14. When we compared the IPSCs between cells recorded from P12 to P14 and P16 to P18 animals, we found no significant shape differences, suggesting that the subunit composition of glycinergic receptors did not change in this age range.

Chloride reversal in CWCs

In a seminal set of studies in P18–P26 mice, the glycinergic and GABAergic events observed in CWCs were depolarizing with reversal potentials of approximately -53 mV (Golding and Oertel 1996, 1997). These results differed from those of Manis et al. (1994), who found that CWCs in adult guinea pigs exhibited inhibitory postsynaptic potentials, even at -60 mV. The age difference of the animals in these two studies might be responsible for the different results because the reversal potential of glycine- and GABA-mediated events shifts from depolarizing early on in development to hyperpolarizing at later ages (Ehrlich et al. 1999; Kakazu et al. 1999; Kandler and Friauf 1995; Singer et al. 1998). However, in the lateral superior olive, glycine responses have been reported to shift from depolarization to hyperpolarizing as early as P8 (Kandler and Friauf 1995), raising the possibility that the equilibrium potential for Cl^- in cartwheel cells has already shifted in P18–P26 mice. Using perforated-patch recordings that should not disturb intracellular Cl^- , we found that the reversal potential for IPSPs in P10–P11 rats was -67 mV. This value is similar to the reversal potential of glycine evoked currents obtained in neurons of the lateral superior olive between P5 and P15 (Ehrlich et al. 1999; Kakazu et al. 1999; Kandler and Friauf 1995). Our results suggest that CWCs establish a low intracellular chloride level early and that a developmental delay is unlikely to account for an elevated reversal in juvenile mice. Although we did not measure reversal potentials, perforated-patch recordings in two CWCs also showed hyperpolarizing IPSPs at rest in P18–P19 rats (data not shown). Therefore CWCs do not appear to provide feedback excitation to the CWC-CWC network but instead provide inhibition with characteristics that will affect the network in a specific manner (see following text). The discrepancies in the reversal potential of IPSPs in the DCN might, however, be species specific.

Functional significance

Our observations suggest that CWC inhibition plays a dual role in the DCN. Interactions between CWCs are slow and facilitating, which implies that CWC-CWC signaling is “low-pass,” depending more on average rate than on detailed spike timing. On the other hand, CWC-PC inhibition is stronger and faster and shows synaptic depression, which implies that it is “high-pass” and will effectively signal changes in CWC firing rate to PCs. In addition, bursting in CWCs produces a proportionally larger effect in CWC-CWC IPSPs than in CWC-PC IPSPs and is thus more effectively signaled to other CWCs than to PCs. Consequently, bursts may carry different information between CWCs as opposed to their effects on PCs. The time course of IPSPs can also determine the phase at which inhibitory interneurons and their postsynaptic targets fire. Broad IPSPs, as those seen between CWCs, will tend to synchronize the output of a presynaptic cell with its postsynaptic target, while fast IPSPs, such as those seen in PCs, tend to drive the connected cells in anti-synchrony (Di Garbo et al. 2005; Merriam et al. 2005; Wang and Buzsaki 1996). Taken together, these findings support the notion of a dual role for CWC synapses that differentially control firing within the CWC-CWC network as opposed to their feed-forward inhibition of PCs.

GRANTS

This work was supported by the National Institute on Deafness and Other Communications Diseases Grant R01 DC-000425 to P. B. Manis.

REFERENCES

- Altschuler RA, Betz H, Parakkal MH, Reeks KA, Wenthold RJ. Identification of glycinergic synapses in the cochlear nucleus through immunocytochemical localization of the postsynaptic receptor. *Brain Res* 369: 316–320, 1986.
- Beierlein M, Gibson JR, Connors BW. A network of electrically coupled interneurons drives synchronized inhibition in neocortex. *Nat Neurosci* 3: 904–910, 2000.
- Berberi AS, Mugnaini E. Distribution and targets of the cartwheel cell axon in the dorsal cochlear nucleus of the guinea pig. *Anat Embryol* 183: 427–454, 1991.
- Blackstad TW, Osen KK, Mugnaini E. Pyramidal neurones of the dorsal cochlear nucleus: a Golgi and computer reconstruction study in cat. *Neuroscience* 13: 827–854, 1984.
- Brawer JR, Morest DK, Kane EC. The neuronal architecture of the cochlear nucleus of the cat. *J Comp Neurol* 155: 251–300, 1974.
- Brown MC, Berglund AM, Kiang NY, Ryugo DK. Central trajectories of type II spiral ganglion neurons. *J Comp Neurol* 278: 581–590, 1988.
- Brown MC, Ledwith JV 3rd. Projections of thin (type-II) and thick (type-I) auditory-nerve fibers into the cochlear nucleus of the mouse. *Hear Res* 49: 105–118, 1990.
- Campos ML, de Cabo C, Wisden W, Juiz JM, Merlo D. Expression of GABA(A) receptor subunits in rat brainstem auditory pathways: cochlear nuclei, superior olivary complex and nucleus of the lateral lemniscus. *Neuroscience* 102: 625–638, 2001.
- Clements JD, Bekkers JM. Detection of spontaneous synaptic events with an optimally scaled template. *Biophys J* 73: 220–229, 1997.
- Davis KA, Young ED. Granule cell activation of complex-spiking neurons in dorsal cochlear nucleus. *J Neurosci* 17: 6798–6806, 1997.
- Di Garbo A, Panarese A, Chillemi S. Gap junctions promote synchronous activities in a network of inhibitory interneurons. *Biosystems* 79: 91–99, 2005.
- Dugue GP, Dumoulin A, Triller A, Dieudonne S. Target-dependent use of co-released inhibitory transmitters at central synapses. *J Neurosci* 25: 6490–6498, 2005.
- Ehrlich I, Lohrke S, Friauf E. Shift from depolarizing to hyperpolarizing glycine action in rat auditory neurones is due to age-dependent Cl^- regulation. *J Physiol* 520: 121–137, 1999.

- Golding NL, Oertel D.** Context-dependent synaptic action of glycinergic and GABAergic inputs in the dorsal cochlear nucleus. *J Neurosci* 16: 2208–2219, 1996.
- Golding NL, Oertel D.** Physiological identification of the targets of cartwheel cells in the dorsal cochlear nucleus. *J Neurophysiol* 78: 248–260, 1997.
- Juiz JM, Helfert RH, Wenthold RJ, De Blas AL, Altschuler RA.** Immunocytochemical localization of the GABA_A/benzodiazepine receptor in the guinea pig cochlear nucleus: evidence for receptor localization heterogeneity. *Brain Res* 504: 173–179, 1989.
- Kakazu Y, Akaike N, Komiyama S, Nabekura J.** Regulation of intracellular chloride by cotransporters in developing lateral superior olive neurons. *J Neurosci* 19: 2843–2851, 1999.
- Kaltenbach JA.** Summary of evidence pointing to a role of the dorsal cochlear nucleus in the etiology of tinnitus. *Acta Otolaryngol Suppl* 556: 20–26, 2006.
- Kandler K, Friauf E.** Development of glycinergic and glutamatergic synaptic transmission in the auditory brainstem of perinatal rats. *J Neurosci* 15: 6890–6904, 1995.
- Kane EC.** Synaptic organization in the dorsal cochlear nucleus of the cat: a light and electron microscopic study. *J Comp Neurol* 155: 301–329, 1974.
- Kanold PO, Young ED.** Proprioceptive information from the pinna provides somatosensory input to cat dorsal cochlear nucleus. *J Neurosci* 21: 7848–7858, 2001.
- Kim Y, Trussell LO.** Ion channels generating complex spikes in cartwheel cells of the dorsal cochlear nucleus. *J Neurophysiol* 97: 1705–1725, 2007.
- Kolston J, Osen KK, Hackney CM, Ottersen OP, Storm-Mathisen J.** An atlas of glycine- and GABA-like immunoreactivity and colocalization in the cochlear nuclear complex of the guinea pig. *Anat Embryol* 186: 443–465, 1992.
- Lohrke S, Srinivasan G, Oberhofer M, Doncheva E, Friauf E.** Shift from depolarizing to hyperpolarizing glycine action occurs at different perinatal ages in superior olivary complex nuclei. *Eur J Neurosci* 22: 2708–2722, 2005.
- Lu T, Rubio ME, Trussell LO.** Glycinergic transmission shaped by the corelease of GABA in a mammalian auditory synapse. *Neuron* 57: 524–535, 2008.
- Manis PB.** Membrane properties and discharge characteristics of guinea pig dorsal cochlear nucleus neurons studied in vitro. *J Neurosci* 10: 2338–2351, 1990.
- Manis PB, Brownell WE.** Synaptic organization of eighth nerve afferents to cat dorsal cochlear nucleus. *J Neurophysiol* 50: 1156–1181, 1983.
- Manis PB, Spirou GA, Wright DD, Paydar S, Ryugo DK.** Physiology and morphology of complex spiking neurons in the guinea pig dorsal cochlear nucleus. *J Comp Neurol* 348: 261–276, 1994.
- Merriam EB, Netoff TI, Banks MI.** Bistable network behavior of layer I interneurons in auditory cortex. *J Neurosci* 25: 6175–6186, 2005.
- Molitor SC, Manis PB.** Dendritic Ca²⁺ transients evoked by action potentials in rat dorsal cochlear nucleus pyramidal and cartwheel neurons. *J Neurophysiol* 89: 2225–2237, 2003.
- Oertel D, Wu SH.** Morphology and physiology of cells in slice preparations of the dorsal cochlear nucleus of mice. *J Comp Neurol* 283: 228–247, 1989.
- Oertel D, Young ED.** What's a cerebellar circuit doing in the auditory system? *Trends Neurosci* 27: 104–110, 2004.
- Ohlrogge M, Doucet JR, Ryugo DK.** Projections of the pontine nuclei to the cochlear nucleus in rats. *J Comp Neurol* 436: 290–303, 2001.
- Osen KK.** Cytoarchitecture of the cochlear nuclei in the cat. *J Comp Neurol* 136: 453–484, 1969.
- Piechotta K, Weth F, Harvey RJ, Friauf E.** Localization of rat glycine receptor alpha1 and alpha2 subunit transcripts in the developing auditory brainstem. *J Comp Neurol* 438: 336–352, 2001.
- Portfors CV, Roberts PD.** Temporal and frequency characteristics of cartwheel cells in the dorsal cochlear nucleus of the awake mouse. *J Neurophysiol* 98: 744–756, 2007.
- Reyes A, Lujan R, Rozov A, Burnashev N, Somogyi P, Sakmann B.** Target-cell-specific facilitation and depression in neocortical circuits. *Nat Neurosci* 1: 279–285, 1998.
- Rhode WS, Smith PH.** Physiological studies on neurons in the dorsal cochlear nucleus of cat. *J Neurophysiol* 56: 287–307, 1986.
- Rhode WS, Smith PH, Oertel D.** Physiological response properties of cells labeled intracellularly with horseradish peroxidase in cat dorsal cochlear nucleus. *J Comp Neurol* 213: 426–447, 1983.
- Roberts MT, Bender KJ, Trussell LO.** Fidelity of complex spike-mediated synaptic transmission between inhibitory interneurons. *J Neurosci* 28: 9440–9450, 2008.
- Rubio ME, Juiz JM.** Differential distribution of synaptic endings containing glutamate, glycine, and GABA in the rat dorsal cochlear nucleus. *J Comp Neurol* 477: 253–272, 2004.
- Ryugo DK, May SK.** The projections of intracellularly labeled auditory nerve fibers to the dorsal cochlear nucleus of cats. *J Comp Neurol* 329: 20–35, 1993.
- Sato K, Kuriyama H, Altschuler RA.** Expression of glycine receptor subunits in the cochlear nucleus and superior olivary complex using non-radioactive in situ hybridization. *Hear Res* 91: 7–18, 1995.
- Sato K, Kuriyama H, Altschuler RA.** Expression of glycine receptor subunit mRNAs in the rat cochlear nucleus. *Hear Res* 144: 47–52, 2000.
- Shore SE.** Multisensory integration in the dorsal cochlear nucleus: unit responses to acoustic and trigeminal ganglion stimulation. *Eur J Neurosci* 21: 3334–3348, 2005.
- Shore SE, Moore JK.** Sources of input to the cochlear granule cell region in the guinea pig. *Hear Res* 116: 33–42, 1998.
- Shore SE, Zhou J.** Somatosensory influence on the cochlear nucleus and beyond. *Hear Res* 216: 217: 90–99, 2006.
- Singer JH, Talley EM, Bayliss DA, Berger AJ.** Development of glycinergic synaptic transmission to rat brain stem motoneurons. *J Neurophysiol* 80: 2608–2620, 1998.
- Thompson AM, Thompson GC.** Serotonin projection patterns to the cochlear nucleus. *Brain Res* 907: 195–207, 2001.
- Wang XJ, Buzsaki G.** Gamma oscillation by synaptic inhibition in a hippocampal interneuronal network model. *J Neurosci* 16: 6402–6413, 1996.
- Weedman DL, Ryugo DK.** Pyramidal cells in primary auditory cortex project to cochlear nucleus in rat. *Brain Res* 706: 97–102, 1996.
- Weinberg RJ, Rustioni A.** A cuneocochlear pathway in the rat. *Neuroscience* 20: 209–219, 1987.
- Wenthold RJ, Zempel JM, Parakkal MH, Reeks KA, Altschuler RA.** Immunocytochemical localization of GABA in the cochlear nucleus of the guinea pig. *Brain Res* 380: 7–18, 1986.
- Wouterlood FG, Mugnaini E.** Cartwheel neurons of the dorsal cochlear nucleus: a Golgi-electron microscopic study in rat. *J Comp Neurol* 227: 136–157, 1984.
- Zhang S, Oertel D.** Cartwheel and superficial stellate cells of the dorsal cochlear nucleus of mice: intracellular recordings in slices. *J Neurophysiol* 69: 1384–1397, 1993.
- Zhang S, Oertel D.** Neuronal circuits associated with the output of the dorsal cochlear nucleus through fusiform cells. *J Neurophysiol* 71: 914–930, 1994.
- Zhou J, Shore S.** Projections from the trigeminal nuclear complex to the cochlear nuclei: a retrograde and anterograde tracing study in the guinea pig. *J Neurosci Res* 78: 901–907, 2004.